



Original article

# Deciphering the Astigmatic Code in Libyan Keratoconus: From Epidemiological Trends to Clinical Precision

Wael Saadeddin<sup>1\*</sup>, Abdulbari Alshareef<sup>2</sup><sup>1</sup>Department of Ophthalmology, School of Medical Science, Tripoli Academy, Tripoli, Libya<sup>2</sup>Department of Ophthalmology, University of Zawia, Zawia, LibyaCorresponding email: [waelasadadeen@gmail.com](mailto:waelasadadeen@gmail.com)

## Abstract

Keratoconus is a progressive corneal ectasia that typically begins in adolescence, causing irregular astigmatism and visual impairment; in Libya, high consanguinity rates and intense ultraviolet exposure amplify its prevalence and severity, yet local epidemiological data have been lacking. This retrospective cross-sectional study mapped tomographic astigmatism in 1,824 eyes from 955 consecutive patients presenting to ophthalmic centers in Az-Zawiyah between August 2024 and August 2025, using the Sirius+ Scheimpflug-Placido topographer after excluding 86 eyes for incomplete data or other corneal abnormalities. Astigmatism correlated positively with keratoconus severity ( $r_s = 0.278$ ,  $p < 0.001$ ), with each additional diopter increasing diagnostic odds by 83% (OR 1.83, 95% CI 1.68–1.99) and compounding to approximately 11-fold at +4.00 D above baseline; ROC analysis yielded AUC 0.736 (95% CI 0.705–0.768,  $p < 0.001$ ), identifying -3.15 D as the threshold where manifest keratoconus probability becomes clinically dominant. These findings establish astigmatism as a practical triage tool in resource-limited settings, though its low sensitivity for subclinical disease underscores the need for combined other tomographic issues.

**Keywords.** Keratoconus, Corneal Astigmatism, Epidemiology, Libya, Scheimpflug Tomography.

## Introduction

Keratoconus represents a progressive, bilateral, and typically asymmetric corneal ectatic disorder characterized by focal stromal weakening, progressive thinning, and anterior protrusion, with clinical onset most commonly observed during adolescence or early adulthood. The resulting irregular astigmatism degrades vision during formative years—schooling, early employment, family establishment—when demands on sight are greatest [1]. Men and women are affected equally. A meta-analysis of more than 50 million individuals found a global prevalence of 138 per 100,000 (0.138%) [2]. Regional figures diverge: 8.9% in some Middle Eastern cohorts [3] and 7.9% across Africa [4]. These are likely underestimates. Modern tomography detects subclinical and early disease that earlier methods missed, and MENA-specific meta-analyses now report prevalence of 2–3% in certain groups—substantially above Western estimates [5].

Libya represents an extreme within this gradient; consanguinity rates are among the highest worldwide, so there is more autosomal recessive risk. The climate is hot, dry, and intensely ultraviolet-rich, with endemic allergic conjunctivitis and chronic eye rubbing as well [6,7]. These factors converge: KC presents earlier and progresses more rapidly here than in temperate settings. Yet no large cohort has quantified corneal parameters in Libya. In clinical practice, astigmatism is the most accessible screening parameter—an early signal that warrants closer inspection. Yet its ubiquity complicates interpretation: most astigmatism is physiologic, not pathologic. The challenge lies in distinguishing between them. Other studies linked steeper astigmatism to KC before us [8–10]. But where exactly does normal end? No one agrees—cut-offs shift by population [11,12]. We moved to Scheimpflug because Placido only sees the surface. Scheimpflug sees front and back [13,14]. Our machine is the Sirius+ (CSO, Florence)—one pass, both technologies. Thickness, elevation, curvature: all mapped [15,16]. The device generates all these diagnostic indices, but anterior astigmatism retains its primacy as the initial clinical variable. It is the first parameter noted on routine examination, and the one most readily available in settings without tomographic capability.

Tomographic classification, however precise the hardware, depends ultimately on normative comparison. Current device databases derive primarily from European and North American cohorts. Their applicability to Middle Eastern and North African populations—where baseline corneal thickness, curvature, and astigmatism may differ substantially—has not been validated. Without population-specific calibration, the risk of misclassification rises: false positives generate unnecessary referrals and patient anxiety; false negatives delay intervention in progressive disease. Neither outcome is acceptable in a high-prevalence setting. Establishing local normative data is therefore a priority. Recalibrated thresholds would reduce both over-referral and missed diagnosis, aligning screening protocols with the population they serve. We designed this study to define astigmatism distribution in a Libyan clinical cohort and to quantify its relationship with KC severity. Using retrospective data from 1,824 eyes examined at our center in Az-Zawiyah over one year, we sought to establish region-specific thresholds that could inform clinical decision-making in similar practice settings.

## Methods

This retrospective study analyzed existing clinical records from August 2024 to August 2025. Patient identifiers were removed before analysis; data were fully anonymized with no possibility of re-identification. Institutional review board approval was not sought, given the retrospective design and use of historical de-identified data.

Data were collected from consecutive patients presenting to two ophthalmic centers in Az-Zawiyah, Libya, between August 2024 and August 2025. The region is characterized by high ultraviolet exposure and a population with elevated consanguinity rates—factors that elevate baseline KC risk. Most patients presented for routine refractive evaluation, including laser vision correction screening, or reported progressive visual instability. Of 1,910 eyes identified from 955 patients, 86 were excluded following manual review of scan quality. Exclusion criteria were: inadequate topographic data, poor centration, other corneal problems, or significant shadowing from eyelid or lash artifacts. The final analytic sample comprised 1,824 eyes. This deliberate quality filter was applied to ensure that subsequent analyses reflected valid corneal measurements rather than artefactual noise.

Corneal imaging was performed using the Sirius+ system (CSO, Florence, Italy), which combines a rotating Scheimpflug camera with Placido disc topography. This configuration permits simultaneous acquisition of anterior and posterior corneal surfaces, pachymetry, and elevation data. Repeatability was optimized through standardized patient positioning and acquisition protocols.

Eyes were classified into four diagnostic categories based on integrated topographic and tomographic indices: Normal — stable anterior and posterior corneal architecture without ectatic features; Manifest Keratoconus — definitive ectatic changes with consistent topographic signs; Borderline — subtle irregularities falling below formal KC criteria but exceeding normal variation; Other — corneal conditions unrelated to ectasia, maintained as a separate category to preserve the integrity of the primary three-group comparison. The distribution of corneal astigmatism was non-normal; therefore, Spearman's rank correlation coefficient ( $\rho$ ) was used to assess the relationship between astigmatism magnitude and diagnostic category severity. Astigmatism ranged from 0.00 D to -14.11 D across the cohort. To quantify risk at clinically relevant thresholds, we fitted a binary logistic regression model with diagnostic outcome (borderline or manifest KC versus normal) as the dependent variable and astigmatism magnitude as the independent predictor. Results are expressed as Odds Ratios (OR) with 95% Confidence Intervals (CI). An OR of 1.83 per diopter, for example, indicates that each additional diopter of astigmatism increases the odds of KC classification by 83%. All analyses were conducted in IBM SPSS version 26. Statistical significance was set at  $p < 0.05$ .

## Results

### Study Population

Of 1,910 eyes from consecutive patients, 86 (4.5%) were excluded: 42 (2.2%) for suboptimal image quality or acquisition artifact, and 44 (2.3%) for corneal conditions unrelated to ectasia. The remaining 1,824 eyes formed the analytic cohort. The mean patient age was  $22.5 \pm 9.9$  years.

(Table 1) summarizes the distribution. Normal eyes comprised the majority (71.2%,  $n = 1,330$ ). Manifest KC was identified in 17.3% ( $n = 324$ ), and borderline cases in 9.1% ( $n = 170$ ). The remainder had other corneal diagnoses and were retained as a separate category.

**Table 1: The basic topographic characteristics of the samples**

Diagnostic Category	Frequency (n)	Valid Percent (%)	Mean Astigmatism (D)	Std. Deviation ( $\pm$ )
Normal (No KC)	1,330	71.2%	-2.21	1.28
Manifest KC	324	17.3%	-4.08	2.57
Borderline	170	9.1%	-2.13	1.38
Total	1824	100%	-2.54	1.76

Mean astigmatism differed markedly across categories (Table 1). Normal eyes and borderline cases were similar ( $-2.21 \pm 1.28$  D and  $-2.13 \pm 1.38$  D, respectively). In manifest KC, the mean shifted to  $-4.08 \pm 2.57$  D (range 0.00 to -14.11 D). This near-doubling aligns with the regression finding that each additional diopter of astigmatism increases KC odds by approximately 83%. The ROC analysis (AUC 0.736, 95% CI 0.705–0.768) identified -3.15 D as the threshold balancing sensitivity and specificity (cut-off point). Below this value, astigmatism likely reflects physiologic variation; above it, ectasia probability rises sufficiently to justify tomographic referral.

### Comparative Analysis

The Kruskal-Wallis test rejected the null hypothesis of equal distributions across groups ( $p < 0.001$ , Table 2). Pairwise comparisons (Figure 1) showed that manifest KC differed from both normal and borderline

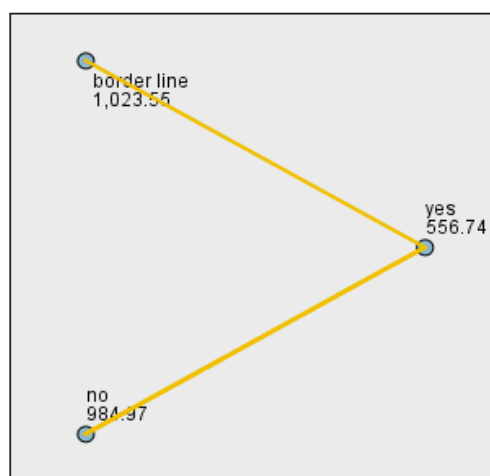
eyes ( $p < 0.001$  for both). The normal and borderline groups, however, did not differ significantly ( $p = 1.000$ ).

**Table 2: Hypothesis Test Summary revealing Rejection of the null hypothesis**

<b>Hypothesis Test Summary</b>				
	Null Hypothesis	Test	Sig.	Decision
1	The distribution of the negative sign is the same across categories of KC.	Independent-Samples Kruskal-Wallis Test	.000	Reject the null hypothesis.
Asymptotic significances are displayed. The significance level is .05.				

Post-hoc pairwise comparisons localized these differences (Figure 1). Manifest KC differed from normal and borderline eyes (both  $p < 0.001$ ). The normal and borderline groups, however, were statistically indistinguishable ( $p = 1.000$ ). This overlap is clinically relevant: in early ectasia, astigmatism magnitude may remain within the physiologic range, delaying recognition.

**Pairwise Comparisons of KC**



Each node shows the sample average rank of KC.

Sample1-Sample2	Test Statistic	Std. Error	Std. Test Statistic	Sig.	Adj.Sig.
yes-no	428.237-	32.630	13.124-	.000	.000
yes-border line	466.811-	49.879	9.359-	.000	.000
no-border line	38.574-	42.899	.899-	.369	1.000

Each row tests the null hypothesis that the Sample 1 and Sample 2 distributions are the same. Asymptotic significances (2-sided tests) are displayed. The significance level is .05.

**Figure 1. Pairwise Comparisons of Diagnostic Groups.**

Post-hoc analysis reveals significant differences between Manifest KC and other groups ( $p < 0.001$ ), while no significant difference exists between Normal and Borderline cohorts (Adj.  $p = 1.000$ ).

Chi-square analysis confirmed the association between astigmatism magnitude and diagnostic category ( $\chi^2 = 125.439$ ,  $df = 2$ ,  $p < 0.001$ ). Stratifying by threshold:

- Astigmatism  $\leq -3.15$  D: KC prevalence 33.0% (182 of 552 eyes)
- Astigmatism  $> -3.15$  D: KC prevalence 11.2% (142 of 1,272 eyes)

The high-astigmatism stratum ( $-5.00$  D or steeper) showed the highest KC concentration at 76.7%.

### Visual Representation

(Figure 2) illustrates these distributions. The bar chart (A) shows the stepwise increase in mean astigmatism from normal to manifest KC. The boxplot (B) reveals greater dispersion in the KC group, with outliers extending to  $-14.11$  D, consistent with the heterogeneity of ectatic disease. Normal and borderline eyes cluster more tightly.

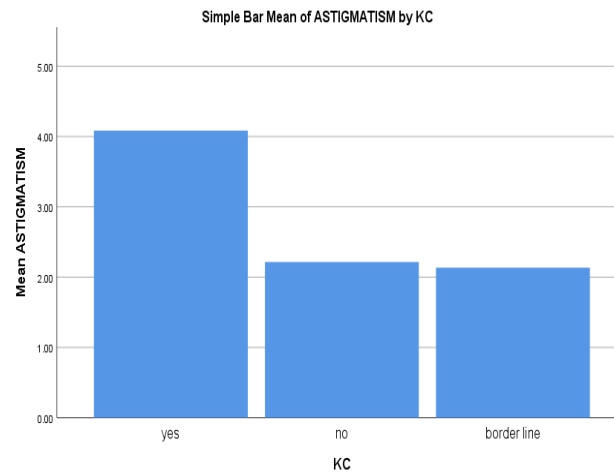


**Figure 2A. Mean Corneal Astigmatism by Group.**

Bar Chart, the bar chart shows a clear elevation in mean astigmatism for the Manifest KC group (> 4.00 D) compared to the Normal and Borderline groups.

Key Finding: The visual similarity between the Normal and Borderline bars supports the post-hoc results ( $p = 1.000$ ), confirming no significant difference between them, while the Manifest KC group stands out as significantly higher.

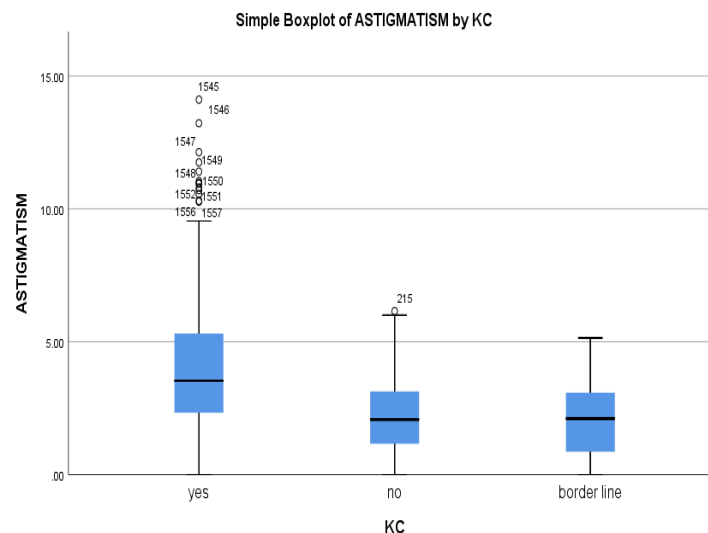


**Figure 2B. Comparison of Astigmatism Magnitude across Diagnostic Groups.**

Boxplot Chart. The boxplot shows a significant upward trend in astigmatism magnitude from Normal to Manifest KC groups. The central horizontal lines represent median values, while the boxes indicate the interquartile range (IQR).

### Correlation and Predictive Modeling

Spearman's rho showed a modest positive correlation between astigmatism magnitude and diagnostic severity ( $r_s = 0.278$ ,  $p < 0.001$ ). The logistic regression model was significant overall ( $\chi^2 = 267.221$ ,  $df = 1$ ,  $p < 0.001$ ). Each additional diopter of astigmatism increased the odds of KC classification by 83% (OR 1.83, 95% CI 1.68–1.99). Nagelkerke  $R^2$  was 0.237, indicating that astigmatism alone explains approximately 24% of diagnostic variance—substantial for a single refractive measure. Model accuracy was 84.5%.

### ROC Analysis

ROC analysis evaluated astigmatism as a classifier for KC versus normal. The AUC was 0.736 (95% CI 0.705–0.768,  $p < 0.001$ ), indicating fair discriminative ability. The confidence interval width (0.063) reflects adequate precision given the sample size.

At -2.80 D, sensitivity was 63.0%, but specificity was only 68.0%. The -3.15 D threshold offered better balance: sensitivity 55.9%, specificity 75.1%. Given the healthy cohort mean of -2.21 D, a cut-off at -3.15 D lies approximately one standard deviation above the physiologic baseline. Eyes exceeding this value warrant tomographic evaluation.

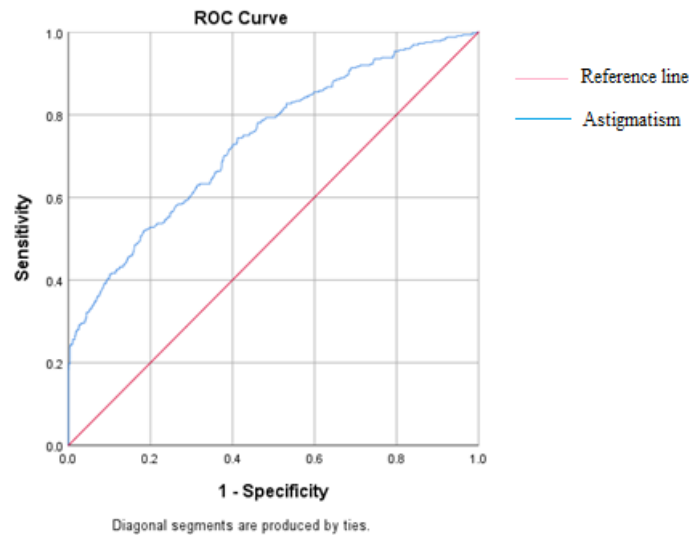


**Figure 3. (ROC) curve analysis to evaluate the discriminatory ability of cylinder power in detecting keratoconus.**

Cylinder power alone demonstrated a moderate discriminatory ability for detecting keratoconus, with an area under the curve of 0.736 (95% CI: 0.705–0.768,  $p < 0.001$ ).

## Discussion

### Astigmatism as a Regional Diagnostic Indicator

In this cohort of 1,824 eyes, astigmatism magnitude correlated positively with KC severity ( $r_s = 0.278$ ,  $p < 0.001$ ). The prevalence gradient was steep: 11.2% with astigmatism milder than  $-3.15$  D, 33.0% at  $-3.15$  D or steeper, and 76.7% at  $-5.00$  D or steeper. These figures match prior reports linking astigmatism to KC [10,17,18]. In our cohort, the relationship was degree-dependent: 33.0% of eyes at  $-3.15$  D or steeper had KC, rising to 76.7% at  $-5.00$  D or beyond. A  $-3.15$  D threshold may serve as a practical triage point in Libyan clinics, where tomography is not universally available. Each additional diopter of astigmatism was associated with 1.83 times the odds of KC

(OR 1.83, 95% CI 1.68–1.99,  $p < 0.001$ ). Safir et al reported a close increment (OR 1.75, 95% CI 1.69–1.80,  $p < 0.001$ ) [19]. The multiplicative effect is shown in Figure 4: cumulative odds reach 11.19-fold at  $+4.00$  D. In this population, where advanced KC often presents late, a 4-D shift carries clinical weight. Rapid progression in young patients warrants particular attention. Astigmatic shifts exceeding 1 D per year should prompt Scheimpflug imaging to exclude ectasia [1]. Refractive management without tomographic assessment risks missing structural disease.

Exponential Risk Escalation of Keratoconus in the Libyan Population  
(Based on Logistic Regression Model:  $\text{Exp}(B) = 1.829$ )

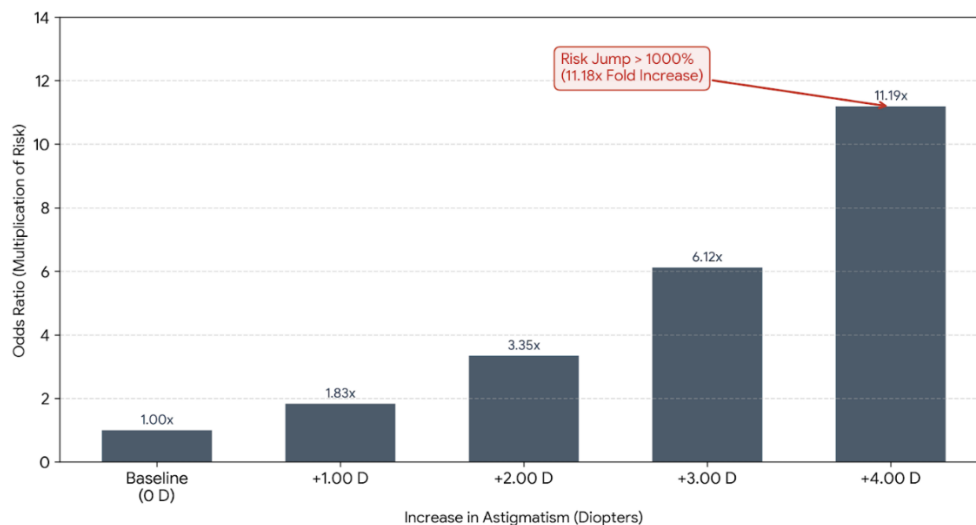


**Figure 4. Compounding keratoconus risk with increasing astigmatism. Each additional diopter multiplies baseline odds by 1.83; a 4 D shift yields an approximately 11-fold risk elevation.**

### **The Borderline Diagnostic Gap**

The statistical overlap between normal and borderline eyes ( $p = 1.000$ ) is not a measurement artifact but a genuine clinical phenomenon. Early ectasia may alter posterior corneal elevation and stromal thickness distribution before anterior astigmatism deviates from the physiologic range. Bae et al. demonstrated this sequence in fellow eyes of unilateral KC: posterior abnormalities preceded anterior topographic change in a substantial proportion of cases [20]. In our setting, a normal or mildly elevated cylinder value does not exclude early disease. Screening limited to anterior astigmatism will miss subclinical cases. Posterior elevation mapping and pachymetry—available on the Sirius+ platform—are necessary adjuncts, particularly for patients with atopic disease, family history, or subjective visual fluctuation.

### **Regional Dynamics and Public Health Impact**

The quantified risk gradient supports structured triage in high-volume settings. Patients with astigmatism exceeding  $-3.15$  D, or those showing rapid progression, can be flagged for accelerated evaluation and CXL referral where indicated. Early intervention halts progression in the majority of cases, reducing long-term visual morbidity and the eventual need for keratoplasty. In a region with limited subspecialty access, such a metric helps allocate scarce resources: not every patient needs immediate tomography, but those above the threshold do.

### **Clinical Integration and Comparative Analysis**

Our findings fit with what others have reported. Gordon et al followed patients who developed KC: their astigmatism shifted from  $-1.57$  D early to  $-3.23$  D later [7]. Our mapping in the Libyan population shows a slightly higher 'physiological baseline' for normal eyes (Mean:  $-2.21$  D). This gap suggests that thresholds derived elsewhere may not apply here. The borderline-normal overlap in our data ( $p = 1.000$ ,  $-2.13$  D versus  $-2.21$  D) confirms a known limitation: anterior cylinder misses early disease. Our AUC of  $0.736$  fits this pattern—discriminative, but not diagnostic.

The  $\sim 11$ -fold risk at  $+4.00$  D sounds dramatic, yet it describes association, not prediction. Kim et al. found mean astigmatism of  $3.05$  D in 64 KC patients—below our threshold, consistent with progressive rather than early disease [21]. Safir et al. reported AUC  $0.752$  (95% CI  $0.740$ – $0.763$ ) with a cut-off of  $2.88$  D (sensitivity  $74.4\%$ , specificity  $64.4\%$ ); modest numbers that warn against using astigmatism alone [19]. Garcia-Ferrer et al. and Gomes et al. [8,1] made this explicit: eye rubbing, atopic disease, family history—clinical context matters as much as the cylinder.

### **Methodological Insights and Future Research Opportunities**

The normal-borderline overlap may reflect heterogeneity in our broad cohort rather than true biological equivalence. Variance in astigmatism magnitude—ranging from  $0.00$  to  $-14.11$  D—can obscure subtle morphological distinctions in early disease. Restricting analysis to eyes with low-magnitude astigmatism ( $< -2.00$  D) could reduce this variance and clarify whether a subtler threshold exists for subclinical detection. Future work should also incorporate posterior elevation and corneal hysteresis to capture structural change before anterior astigmatism shifts.

### **The Diagnostic Profile: Specificity vs. Sensitivity**

Astigmatism in this cohort showed a specificity of  $98.9\%$  and sensitivity of  $25.0\%$  at the  $-3.15$  D threshold. This profile characterizes it as an effective rule-out test: a patient below the threshold has a  $99\%$  probability of a normal cornea, minimizing unnecessary referral. However, the low sensitivity confirms that astigmatism is a late indicator; early ectasia often manifests with posterior elevation change or pachymetric thinning before the anterior cylinder deviates. Therefore, astigmatism should not stand alone as a screening tool but rather trigger tomographic evaluation—posterior elevation and thickness mapping—to capture disease at a subclinical stage.

### **Limitations and Future Directions**

This analysis is cross-sectional; it defines risk at a single time point rather than tracking progression. The per-diopter odds increment (OR  $1.83$ ) describes association, not trajectory. Longitudinal cohort studies are needed to establish rates of change in this population and to determine whether age modifies the astigmatism-KC relationship. Such designs would also clarify which normal-appearing corneas progress to ectasia over time.

Measurement repeatability may be reduced in advanced KC due to corneal irregularity, introducing variability that could affect classification. We did not control for ocular surface disease, which may influence keratometry and introduce measurement bias. Higher-order aberrations, integrated with tomographic data, may improve sensitivity for subclinical disease in future models.

### **Conclusion**

In this Libyan cohort, corneal astigmatism showed a graded relationship with KC severity: each 1-diopter increase was associated with a  $1.83$ -fold higher likelihood of keratoconus (OR  $1.83$ ), and the  $-3.15$  D threshold offered fair discriminative value (AUC  $0.736$ , sensitivity  $55.9\%$ , specificity  $75.1\%$ ). These findings

support astigmatism as a first-line triage tool in settings where tomography is not immediately available—not as a standalone diagnostic test. The limitation is fundamental: the normal-borderline overlap ( $p = 1.000$ ) demonstrates that substantial ectatic change may precede anterior cylinder deviation, and the low sensitivity (25.0%) at this threshold confirms that astigmatism alone misses early disease. Effective screening requires a combined assessment: astigmatism to flag advanced or progressive disease, posterior elevation, and pachymetry maps to capture subclinical change.

**Conflict of interest.** Nil

## References

- Gomes JAP, Tan D, Rapuano CJ, Belin MW, Ambrósio R, Guell JL, et al. Global consensus on keratoconus and ectatic diseases. *Cornea*. 2015 Apr;34(4):359-69.
- Lucas SEM, Burdon KP. Genetic and environmental risk factors for keratoconus. *Annu Rev Vis Sci*. 2020 Sep 15;6:25-46.
- Sidky MK, Hassanein DH, Eissa SA, Salah YM, Lotfy NM. Prevalence of subclinical keratoconus among pediatric Egyptian population with astigmatism. *Clin Ophthalmol*. 2020 Mar 12;14:905-13.
- Akowuah PK, Kobia-Acquah E, Donkor R, Adjei-Anang J, Ankamah-Lomotey S. Keratoconus in Africa: a systematic review and meta-analysis. *Ophthalmic Physiol Opt*. 2021 Jul;41(4):736-47.
- Hashemi H, Heydarian S, Hooshmand E, Saatchi M, Yekta A, Aghamirsalim M, et al. The prevalence and risk factors for keratoconus: a systematic review and meta-analysis. *Cornea*. 2020 Feb;39(2):263-70.
- Gordon-Shaag A, Millodot M, Shneor E, Liu Y. The genetic and environmental factors for keratoconus. *Biomed Res Int*. 2015;2015:795738.
- Gordon-Shaag A, Millodot M, Shneor E. The epidemiology and etiology of keratoconus. *Int J Keratoconus Ectatic Corneal Dis*. 2012 Apr;1(1):7-15.
- Garcia-Ferrer FJ, Akpek EK, Amescua G, Farid M, Lin A, Rhee MK, et al. Corneal Ectasia Preferred Practice Pattern®. *Ophthalmology*. 2019 Jan;126(1):P170-215.
- Zhao SH, Berkowitz C, Ralay Ranaivo H, Laurenti K, Bohnsack BL, Basti S, et al. Evaluation of parameters for early detection of pediatric keratoconus. *BMC Ophthalmol*. 2024 Oct 21;24(1):463.
- Choi Y, Eom Y, Song JS, Kim HM. Comparison of anterior, posterior, and total corneal astigmatism measured using a single Scheimpflug camera in healthy and keratoconus eyes. *Korean J Ophthalmol*. 2018 Jun;32(3):163-71.
- Atalay E, Özalp O, Erol MA, Bilgin M, Yıldırım N. A combined biomechanical and tomographic model for identifying cases of subclinical keratoconus. *Cornea*. 2020 Apr;39(4):461-7.
- Abtahi MA, Beheshtnejad AH, Latifi G, Akbari-Kamrani M, Ghafarian S, Masoomi A, et al. Corneal epithelial thickness mapping: a major review. *J Ophthalmol*. 2024 Jan 2;2024:6674747.
- Savini G, Barboni P, Carbonelli M, Hoffer KJ. Repeatability of automatic measurements by a new Scheimpflug camera combined with Placido topography. *J Cataract Refract Surg*. 2011 Oct;37(10):1809-16.
- Belin MW, Khachikian SS, Ambrósio R Jr. Elevation based corneal tomography. New Delhi: Jaypee-Highlights Medical Publishers; 2012. 252 p.
- Shneor E, Millodot M, Zyroff M, Gordon-Shaag A. Validation of keratometric measurements obtained with a new integrated aberrometry-topography system. *J Optom*. 2012 Apr;5(2):80-6.
- Wallace HB, Vellara HR, Gokul A, McGhee CNJ, Meyer JJ. Comparison of ectasia detection in early keratoconus using Scheimpflug-based corneal tomography and biomechanical assessments. *Cornea*. 2023 Dec;42(12):1528-35.
- Abdul Fattah M, Mireskandari K, Fung SSM, Woo JH, Ali A. Children with high astigmatism: tomographic and refractive characteristics and the ability of current indices to rule out keratoconus. *J AAPOS*. 2023 Dec;27(6):328.e1-328.e7.
- Koppen C, Jiménez-García M, Kreps EO, Ni Dhubhghaill S, Rozema JJ. Definitions for keratoconus progression and their impact on clinical practice. *Eye Contact Lens*. 2024 Jan 1;50(1):1-9.
- Safir M, Nitzan I, Hanina Y, Heller D, Mimouni M, Sorkin N. Keratoconus prevalence in astigmatic adolescents: findings from a nationwide screening setting. *Eye*. 2025 Nov 18;39(16):2958-62.
- Bae GH, Kim JR, Kim CH, Lim DH, Chung ES, Chung TY. Corneal topographic and tomographic analysis of fellow eyes in unilateral keratoconus patients using Pentacam. *Am J Ophthalmol*. 2014 Jan;157(1):103-109.e1.
- Kim J, Whang WJ, Kim HS. Analysis of total corneal astigmatism with a rotating Scheimpflug camera in keratoconus. *BMC Ophthalmol*. 2020 Dec 3;20(1):475.